applied sciences

MDPI

Review

Use of Machine Learning and Remote Sensing Techniques for Shoreline Monitoring: A Review of Recent Literature

Chrysovalantis-Antonios D. Tsiakos * and Christos Chalkias *

Department of Geography, Harokopio University of Athens, 176 76 Kallithea, Greece
* Correspondence: tsiakos@hua.gr (C.-A.D.T.); xalkias@hua.gr (C.C.); Tel.: +30-2109549347 (C.C.)

Abstract: Climate change and its effects (i.e., sea level rise, extreme weather events) as well as anthropogenic activities, determine pressures to the coastal environments and contribute to shoreline retreat and coastal erosion phenomena. Coastal zones are dynamic and complex environments consisting of heterogeneous and different geomorphological features, while exhibiting different scales and spectral responses. Thus, the monitoring of changes in the coastal land classes and the extraction of coastlines/shorelines can be a challenging task. Earth Observation data and the application of spatiotemporal analysis methods can facilitate shoreline change analysis and detection. Apart from remote sensing methods, the advent of machine learning-based techniques presents an emerging trend, being capable of supporting the monitoring and modeling of coastal ecosystems at large scales. In this context, this study aims to provide a review of the relevant literature falling within the period of 2015–2022, where different machine learning approaches were applied for cases of coast-line/shoreline extraction and change analysis, and/or coastal dynamic monitoring. Particular emphasis is given on the analysis of the selected studies, including details about their performances, as well as their advantages and weaknesses, and information about the different environmental data employed.

Keywords: machine learning; geospatial intelligence; earth observation; coastal erosion; shoreline extraction; literature review

check for updates

Citation: Tsiakos, C.-A.D.; Chalkias, C. Use of Machine Learning and Remote Sensing Techniques for Shoreline Monitoring: A Review of Recent Literature. *Appl. Sci.* **2023**, *13*, 3268. https://doi.org/10.3390/app13053268

Academic Editors: Wojciech Zgłobicki and Leszek Gawrysiak

Received: 31 January 2023
Revised: 28 February 2023
Accepted: 1 March 2023
Published: 3 March 2023

Copyright: © 2023 by the authors. Licensee MDPI, Basel, Switzerland. This article is an open access article distributed under the terms and conditions of the Creative Commons Attribution (CC BY) license (https://creativecommons.org/licenses/by/4.0/).

1. Introduction

Coastal environments consist of complex ecosystems, while also being host to species and habitats that provide many benefits to society and natural ecosystems [1]. These environments are being pressured by human activities while also being stressed by climate change and its effects, such as extreme weather events and sea level rise [2]. At the European scale, it is projected that the erosion of sandy coasts due to sea level rise occurring in the deficit of land cover/use will result in a 1400–2500 km^2 coastal land loss by 2100, considering the prevailing scenarios [3]. Usually, monitoring these areas and the associated phenomena is challenging due to their heterogeneous characteristics. In addition, current coastal studies are often limited in time or space, making them difficult to use for short-term regional spatial planning. Therefore, a new national/regional quantitative approach is needed.

Shoreline monitoring, stipulated as the approach allowing for the identification of the intersection between the land and water surfaces, requires a consideration of spatiotemporal elements that underpin the dynamic evolution of land–water boundary conditions [4]. Relevant literature reviews [4,5] illustrate the use of shoreline indicators, acting as a proxy of the coastline water–land boundary conditions, being organized into three main categories: (i) indicators relying on visible coastal distinguishable elements, (ii) indicators based on tidal data, and (iii) indicators employing image processing and analysis techniques towards the extraction of coastline features. The first category of indicators can cover the position of a selected shoreline such as the high-water line (i.e., the high wetting limit occurred by the

last swash) [6,7], the wet/dry line (i.e., the boundary of the dimmer sand) [8,9] and water line defined as the interface between the water and the land [10–12], morphological limits (i.e., cliffs [13–15], dunes [16–19], headwall scarps, or protected seafront structures [20,21]) and/or vegetation limits [22–25]. On the other hand, tidal-datum indicators such as mean high/low water line [26–28] or mean sea level [29] are defined based on vertical profiles shaped by the rise and the fall of the tides in association with the coastal profile, whilst meteo-marine insights to relevant stakeholders can be also provided, calculating the wave flow and height, tide phases, or other extreme events (i.e., storm surges) [30].

During the past few years, different tools and approaches have been used in the service of coastal erosion and coastline change monitoring. The majority of these tools rely on geographic information systems (GIS), including both close-source (i.e., ESRI ArcGIS and Digital Shoreline Analysis System [31]) and open-source software (i.e., QGIS and Open Digital Shoreline Analysis System [32]), allowing users to manage and to generate all the geospatial related information that can be subsequently utilized in the context of other programming environments [32]. In the last decade, approaches regarding shoreline change analysis and detection are oriented towards the spatiotemporal analysis of satellite images of high resolution. Apart from remote sensing methods, the advent of machine learning and artificial intelligence-based techniques presents an emerging trend, being capable of supporting the automated extraction of shorelines at large scales. Such methods can facilitate the analysis of large amounts of complex environmental data, and the identification of patterns and trends that are difficult to discern with conventional means, as well as support the generation of accurate habitat maps and the development of predictive models of how coastal ecosystems will respond to different environmental pressures [5].

However, in comparison to other land applications, a relatively small number of studies are focused on the marine domain, and in particular, to tasks related to coastline detection, mainly due to the diverse coastline morphological features that need to be considered, especially at large-scale monitoring scenarios [33].

In this context, this study aims to highlight and to facilitate the understanding of the different machine learning-driven approaches applied for coastal erosion and shoreline changes monitoring, including details about their performance as well as strengths and weaknesses, as well as the different environmental data employed. To the best of our knowledge, despite the advent of machine learning frameworks and their benefit to such applications, a literature review of the relevant research activities is limited or of narrow scope [34], lacking explicit analysis for this domain, which could indicate gaps and facilitate the uptake of these methods. The study takes also into consideration both earth observation and in situ data that are used for the monitoring and modeling of coastal ecosystems.

2. Data and Methods

2.1. Earth Observation Data

In the past decades, satellite remote sensing has been proven to be a very important and cost-effective tool for environmental monitoring [35]. The continuous provision of satellite imagery, with a high frequency of acquisition and a high spatial and spectral accuracy, facilitates the realization of innovative and scalable solutions at various scales (local, regional, and national scales) [36].

In the framework of satellite-based coastal dynamics monitoring and shoreline/coastline extraction, optical and synthetic-aperture radar (SAR) imagery represent complementary and independent sources of information [37]. When the former is available, the different reflection and absorption properties that the land and sea have in the optical spectral range can be extracted [38], while when the latter is available, the different backscattering properties (in terms of signal intensity, dominant scattering mechanism, and/or statistical distribution) that characterize land and sea can be exploited [39]. In this way, the land and sea boundary can be identified even by simply exploiting the inherent capabilities of those imaging sensors. For instance, optical images facilitate easy interpretation but suffer from limited imaging capabilities, being able to operate only during cloud free days, while SAR images can overcome

such drawbacks of the optical systems, yet at the expense of a more complex interpretation (speckle noise, geometric distortion, etc.). As a result, the joint use of optical and SAR images has a number of advantages, since a specific object or class that is not observable via passive sensor images might be monitored using active sensor images and vice versa due to the nature of the electromagnetic radiation used [40].

Currently, Copernicus constitutes one of the most comprehensive Earth Observation programmes, helping with its missions the European Commission member states to develop environmental policies and to monitor the results. In this context, the European Space Agency (ESA) is developing the Sentinel missions for the operational needs of the Copernicus programme, where they address issues related to the availability of coarse- and medium-resolution imagery [41]. Sentinel-2 is such an earth observation mission from the Copernicus Programme, which systematically acquires optical imagery at high spatial resolution (10 m to 60 m) over land and coastal waters [42]. The mission is currently a constellation with two satellites (Sentinel-2A and Sentinel-2B) supporting a broad range of services and applications such as agricultural monitoring, emergencies management, land cover classification, or water quality [43]. On the other hand, Sentinel-1 is a Synthetic Aperture Radar instrument. It operates C-Band in four exclusive imaging modes with different resolutions (down to 5 m) and coverages (up to 400 km). It provides dual polarization capability, a very short revisit time, and rapid product delivery. The mission is composed of a constellation of two satellites, Sentinel-1A and Sentinel-1B, sharing the same orbital plane. Sentinel-1 has the ability to transmit and to receive the backscatter signal, either with single polarization or with cross-polarization. Sentinel-1 data are sensitive to physical properties such as surface roughness, local topography, and dielectric constant [44].

Apart from Copernicus, other satellite missions also provide valuable datasets for environmental and coastal monitoring applications. Landsat missions make available a long-term archive of optical imagery with Landsat 8 to provide eight 30 m multi-spectral bands, one 15 m panchromatic band, and two 100 m spectral bands in the thermal region and with a revisit time of 16 days [45]. Moreover, the availability of very-high-resolution data can support the realization of more precise applications. For instance, the Pleiades constellation covers the Earth with a repeat cycle of 26 days, and delivers panchromatic and multispectral images at spatial resolutions of 0.5 m and 2 m, respectively [46]. WorldView-2 (eight spectral bands with a 1.84 m resolution and one panchromatic band with 0.46m resolution), WorldView-3 (eight multi-spectral bands in the visible near-infrared region with a 1.24 m resolution, one panchromatic with 0.31 m resolution, and eight bands in the short-wave infrared region with 3.7 m resolution) and WorldView-4 (four multi-spectral bands in the visible near-infrared region with a 1.23 m resolution, and one panchromatic with 0.31 m resolution) satellites also constitute options for very-high resolution imagery [47]. Combining very-high spatial resolution (below one meter) with multi-frame image acquisitions can allow for the monitoring of a diverse range of coastal features [48]. In the context of SAR data alternatives to Sentinel-1, the ALOS PALSAR 2 and TerraSAR-X missions operate in six image acquisition modes with resolutions that range from 3 m to 100 m, and from 0.25 m to 40 m, respectively, and while supporting different scene sizes and polarization modes. The combined use of ascending and descending image pairs via L-band and C-band data can support coastal applications for land–water discrimination [49].

2.2. In Situ Data

In situ data in environmental monitoring can be used to measure various parameters directly at their source. It provides accurate, real-time information about the environment, and helps to identify changes or trends over time [50]. In the context of monitoring applications regarding the coastal environment, in situ data can be used for water quality monitoring, measuring weather conditions, and the monitoring of sediment and benthic parameters [51]. Additionally, in situ data play an important role in coastline/shoreline extraction and coastal erosion monitoring. In situ measurements can be utilized as ground truth information that is used to validate remote sensing data, and to assess the accuracy of

the extracted coastline/shoreline. In situ data also provide information about the current conditions of the coastal area, including the location of the shoreline, the presence of vegetation and other physical features, and water depth, which are essential for detecting changes in the coastal environment. The data collected from in situ sources, such as tide gauges, survey markers, and drones, can be used to monitor coastal erosion, to assess the stability of the coastline, and to identify areas that are influenced by erosion [52].

In situ data can support the development and improvement of machine learning models for coastline/shoreline extraction and coastal erosion monitoring. In situ data can be used to train machine learning models, validate their accuracy, and help to address issues of data scarcity and heterogeneity [53,54].

2.3. Machine Learning

Machine learning is considered as the set of algorithms and methods that can be applied for designing and implementing systems, that learn from data, and that are capable of inferring results and/or deducing patterns from the incoming data [55]. Considering the availability of input data and the desired outcome, machine learning algorithms can be grouped into four main categories: supervised learning, unsupervised learning, semi-supervised learning, and reinforcement learning [56,57].

Supervised machine learning covers algorithms that generate functions that are capable of mapping inputs to outputs, based on their training with labeled data (i.e., by learning from input–output examples). Supervised learning is usually applied for classification (i.e., the process of assigning an object with one (binary classification) or more categories (multiple classification) and regression (i.e., the process of predicting one output (univariate), or multiple ones (multivariate) given different parameters) tasks [58]. Different classification algorithms such as Random Forest [59], Support Vector Machines [60], naive Bayes classifier [61], Decision Trees [62], Logistic Regression [63], and K-Nearest Neighbors [64] have been applied to remote sensing and in situ data, aiming to facilitate the improved understanding and monitoring of the environment. Similarly, regression algorithms such as linear and polynomial regression have been utilized to model continuous variables and to perform predictions [65,66]. Deep learning is another category of supervised machine learning, where the models are trained using artificial neural networks with many hidden layers, which allow the model to learn complex representations of the data. These models can learn to identify patterns and to make predictions based on the input data, much like in other supervised learning algorithms [67].

On the other hand, unsupervised learning is driven from the lack of labeled data that can be used for training, and attempts to identify hidden patterns and similarities in the data [56]. Unsupervised learning is usually applied for clustering tasks. Some of the most commonly used algorithms include k-means clustering [68,69] and ISODATA [58,70,71].

Aiming to address the drawbacks of both supervised and unsupervised techniques, semi-supervised learning approaches have been introduced, exploiting both labeled and unlabeled data for training [72]. The unlabeled examples are initially clustered by the supervised algorithm while considering the labeled ones. Then, both the original and newly labeled examples are utilized using the supervised learning algorithm. The overall objective is to minimize the distance between the clusters and the input vectors (in the case of the unlabeled examples), as well as the errors between the target labels and the computed ones (in the case of the labeled examples) [73].

Reinforcement learning constitutes another category of techniques that learn by interacting with the environment. Such algorithms have any prior knowledge regarding the actions to be taken under a specific situation, and thus the learning agent is receiving a reward or a penalty from the environment as a judgement of the applied action. The goal is to minimize penalties and to maximize rewards. Reinforcement learning is not focused on a particular domain rather than on EO data acquisition tasks, and thus it is not expected to be covered in the context of this analysis [57].

2.4. Search Strategy

As part of this systematic literature review procedure, a search of peer-reviewed journals took place in the electronic literature databases of Scopus and Web of Science (WOS), while excluding the grey literature (conference papers, presentations, commentary, extended abstracts, etc.). Boolean operators combining multiple keywords prominent to the research topic, are presented in Table 1 and were queried in the aforementioned database.

Table 1. Group of the selected keywords used in the selected database.

Search Terms
("machine learning" OR "artificial intelligence") AND ("coastal erosion" OR "coastline" OR "shoreline" OR "coastal mapping" OR "shoreline mapping" OR "coastline mapping" OR "coastline change" OR "shoreline change" OR "shoreline extraction" OR "coastline change") AND ("remote sensing" OR "Earth Observation")

A total number of 78 papers were retrieved and evaluated in terms of their relevance with the scope of this study. The above-mentioned figure is in line with the bibliometric analysis performed within 2022 by Ankrah et al. [5], indicating that approximately 5.1% from a total number of 1578 articles that were examined, involve the use of machine learning tools for shoreline change analysis, whilst only 57 papers were published from 2013 and until the first trimester of 2022.

Out of this number, 36 papers and studies were selected and analyzed, covering the period between 2015 and 2022 (Table 2). The selection of the papers was conducted based on their relevance, aiming to cover different cases of coastline/shoreline extraction and change analysis, and/or coastal dynamics monitoring.

Table 2. List of selected papers/studies considered in the context of the study.

Paper/Study Title	Authors
Coastline detection in satellite imagery: A deep learning approach on new benchmark data	Seale et al. (2022) [33]
Multispectral satellite imagery and machine learning for the extraction of shoreline indicators	McAllister et al. (2022) [34]
Evaluating the impacts of major cyclonic catastrophes in coastal Bangladesh using geospatial techniques	Rahaman et al. (2021) [74]
Spatial–Temporal Land Loss Modeling and Simulation in a Vulnerable Coast: A Case Study in Coastal Louisiana	Yang et al. (2022) [75]
Leveraging the Historical Landsat Catalog for a Remote Sensing Model of Wetland Accretion in Coastal Louisiana	Jensen et al. (2022) [76]
Remote sensing and GIS analysis for mapping spatio-temporal changes of erosion and deposition of two Mediterranean river deltas: The case of the Axios and Aliakmonas rivers, Greece	Petropoulos et al. (2015) [77]
Coastal erosion detection using Landsat satellite imagery and support vector machine algorithm	Schellekens and Amani (2022) [78]
Shoreline extraction from WorldView2 satellite data in the presence of foam pixels using a multispectral classification method	Minghelli et al. (2020) [79]
Assessment of coastal geomorphological changes using multi-temporal Satellite-Derived Bathymetry	Misra and Ramakrishnan (2020) [80]
Global coastal geomorphology—integrating earth observation and geospatial data	Mao et al. (2022) [81]
Efficient sea-land segmentation using seeds learning and edge directed graph cut	Cheng et al. (2016) [82]
Multi-feature sea–land segmentation based on pixel-wise learning for optical remote-sensing imagery	Wang et al. (2017) [83]

Table 2. *Cont.*

Paper/Study Title	Authors
Machine learning and shoreline monitoring using optical satellite images: Case study of the Mostaganem shoreline, Algeria	Bengoufa et al. (2021) [84]
Mapping mangroves extents on the Red Sea coastline in Egypt using polarimetric SAR and high resolution optical remote sensing data	Abdel-Hamid et al. (2018) [85]
Spatiotemporal Mapping and Monitoring of Mangrove Forests Changes From 1990 to 2019 in the Northern Emirates, UAE Using Random Forest, Kernel Logistic Regression and Naive Bayes Tree Models	Elmahdy et al. (2020) [86]
Land cover classification in Mangrove ecosystems based on VHR satellite data and machine learning-An upscaling approach	Toosi et al. (2020) [87]
Hybridization of SLIC and extra tree for object based image analysis in extracting shoreline from medium resolution Satellite images	Syaifulnizam et al. (2018a) [88]
Machine-Learning Functional Zonation Approach for Characterizing Terrestrial–Aquatic Interfaces: Application to Lake Erie	Enguehard et al. (2022) [89]
Machine Learning Approaches for Coastline Extraction from Sentinel-2 Images: K-Means and K-Nearest Neighbor Algorithms in Comparison	Alcaras et al. (2022) [90]
An Integrated Monitoring System for Coastal and Riparian Areas Based on Remote Sensing and Machine Learning	Tzepkenlis et al. (2022) [91]
Assessment of coastal variations due to climate change using remote sensing and machine learning techniques: A case study from west coast of India	Pradeep et al. (2022) [92]
Automatic Coastline Extraction Using Edge Detection and Optimization Procedures	Paravolidakis et al. (2018) [93]
Semi-Automated Semantic Segmentation of Arctic Shorelines Using Very High-Resolution Airborne Imagery, Spectral Indices and Weakly Supervised Machine Learning Approaches	Aryal et al. (2021) [94]
Change analysis on historical shorelines extracted from medium resolution satellite images: A case study on the southern coast of Peninsular Malaysia	Syaifulnizam et al. (2018b) [95]
Majority voting of ensemble classifiers to improve shoreline extraction of medium resolution satellite images	Manaf et al. (2017) [96]
Coast type based accuracy assessment for coastline extraction from satellite image with machine learning classifiers	Celik and Gazioglou (2022) [97]
DeepUNet: A Deep Fully Convolutional Network for Pixel-Level Sea-Land Segmentation	Ruirui et al. (2018) [98]
A Novel Deep Structure U-Net for Sea-Land Segmentation in Remote Sensing Images	Shamsolmoali et al. (2019) [99]
Sea-land Segmentation with Res-UNet and fully connected CRF	Chu et al. (2019) [100]
BS-Net: Using Joint-Learning Boundary and Segmentation Network for Coastline Extraction from Remote Sensing Images	Jing et al. (2021) [101]
SANet: A Sea-Land Segmentation Network Via Adaptive Multiscale Feature Learning	Cui et al. (2021) [102]
Application of deep learning models to detect coastlines and shorelines	Dang et al. (2022) [103]
Assessing the accuracy of Sentinel-2 instantaneous subpixel shorelines using synchronous UAV ground truth surveys	Pucino et al. (2022) [104]
CoastSat: a Google Earth Engine-enabled Python toolkit to extract shorelines from publicly available satellite imagery	Vos et al. (2019) [105]
Monitoring 23 years of shoreline changes of the Zengwun Estuary in Southern Taiwan using time-series Landsat data and edge detection techniques	Tsai (2022) [106]
Moving Toward L-Band NASA-ISRO SAR Mission (NISAR) Dense Time Series: Multipolarization Object-Based Classification of Wetlands Using Two Machine Learning Algorithms	Adeli et al. (2021) [107]

3. Results

3.1. Literature Analysis and Main Findings

Rahaman and Esraz (2021) [74] investigated the socio-economic impact of cyclones in coastal areas through the use of Sentinel 2 and Landsat imagery. Remote sensing indices such as the Normalized Difference Vegetation Index (NDVI), Normalized Difference Water Index (NDWI), and Normalized Difference Built-up Index (NDBI) were used for changes analysis in order to monitor water bodies patterns, whilst a supervised classifier (Maximum Likelihood) was used for land-use classification. The classified imagery was used for monitoring change detection dynamics. Moreover, an unsupervised classification method was also evaluated (ISODATA), whilst desktop software (i.e., ArcGIS, ENVI, ERDAS, etc.) were utilized for pre-processing and spatial analysis tasks. The authors concluded that the coarse resolution of satellite data hindered the more precise change detection and micro-level analysis.

Yang et al. (2022) [75] employed supervised classification models (Logistic Regression, Random Forest, and eXtreme Gradient Boosting), aiming to assess the impacts of 15 selected human and environmental variables on the coastal land loss probability at different time instances. The approach was initiated with an analysis of the spatial and temporal patterns affecting land loss in the area of interest, including the quantification of the model predictors at given time instances, as well as the short- and long-term forecasts. It was seen that the performance of non-linear ensemble models was better than the one of Logistic Regression expressing a linear relationship between coastal loss probability and the variables. However, the approach does not take into consideration climate change related variables, whilst it is acknowledged that the use of additional and of higher resolution satellite data could lead to more reliable/accurate results.

A model relying on EO data towards the estimation of accretion rates in coastal wetlands was introduced by Jensen et al. (2022) [76]. Time series of Landsat data, along with available accretion records for the areas of interest, were employed towards the production of proxy variables that contribute to the phenomenon. These include mean NDVI and total suspended solids estimates within water pixels. A Random Forest regression took place, showcasing a good relationship between the above-mentioned utilized variables, whilst the inclusion of elevation and distance factors further improved the estimations of sediment deposition.

Petropoulos et al. (2015) [77] employed Support Vector Machines for the identification of the spatial patterns of coastline changes. Initially, a binary classification scheme was utilized for the discrimination of land and water classes. Then, a training dataset was shaped from Landsat images through a random sampling strategy, and it was used for the development of a multi-class Support Vector Machine pair-wise classification. The method presented a difference in the order of 5–20%, in comparison to photo-interpretation-based approaches. The difference can be attributed to the fact that the Support Vector Machine approach is not applied on a sub-pixel level, and thus the accuracy of the classifiers is reduced, especially when images with coarse spatial resolution are used. In areas with a larger degree of heterogeneity and diversity, the issue can be even more significant. A similar approach was applied by Schellekens and Amani (2022) [78], using Support Vector Machines on optical coastal imagery to determine the magnitude of coastal erosion, whilst the ArcGIS suite was also applied for the spatial analysis of the extracted shorelines. The ability of the SVM algorithm to efficiently estimate the coastal erosion process was showcased in the study of Minghelli et al. (2020) [79], where the algorithm was compared with other supervised classification methods towards assigning an image into three classes (foam, water, and sand).

Misra et al. (2020) [80] assessed coastal geomorphological changes occurring due to coastal erosion through satellite derived bathymetry. Bathymetry data at different time instances were generated by applying a non-linear machine learning technique of Support Vector Regression while harnessing multispectral Landsat 8 imagery. The method is stated to provide good results, particularly in cases with a limited availability of input data in

comparison with other techniques (i.e., Random Forest model) that need a large amount of data in order to ensure a good convergence. The model results are further confirmed with a shoreline change study performed through GIS software (Digital Shoreline Analysis System). The approach indicates positive results for shallow water depth estimation.

A coastal geomorphological analysis was conducted by Mao et al. (2022) [81] at a global scale, covering Australia, US, and EU. The proposed approach involved the combination of raster data with vectorized descriptors in the context of machine learning models towards the classification of intertidal coastal geomorphic features. The coastline data were derived from OpenStreetMap, which according to the authors, was of adequate accuracy in comparison to coastline extracted from Sentinel 1 data. Various geometrical, spectral, and auxiliary data were extracted from coastlines and earth observation data, as well as other existing data from coastal segments. Six supervised classification methods were evaluated in the context of the analysis, including Support Vector Machine, Neural network, Gaussian Naive Bayes, Decision Tree, Random Forest, and adaptive boosting. Coastal areas around the globe (EU, US, and Australia) were classified as bedrock, beach, and wetland. The model implementation was based on geometrical, spectral, and auxiliary variables, and principal component analysis was applied in order to reduce the geometrical dimensions. Then, each machine learning method was iterated for none to all of the geometrical variables extracted from the PCA analysis, and a balanced accuracy from five-fold cross validation was applied for the selection of the best approach (model and input parameters combinations). The Random Forest model outperformed the rest of the models, and it was the one that was applied for the global coastal classification task. The validation was performed through both the testing and validation datasets (with the latter to be provided from independent sources) achieving an overall good accuracy (85% and 84.7%, respectively). Finally, it was found that geometric variables improved the overall classification accuracy; yet uncertainties and misclassification cases were also observed, due to the lack of accuracy and proper variability of the input data.

Cheng et al. (2016) [82] proposed a graph cut-based supervised method to segment the sea and the land from natural-colored images while clustering the image pixels into superpixels. Then, a superpixel-based Support Vector Machine model was implemented for sea–land segmentation. Given the semantic information in the satellite images, a misclassification of land-based pixels was observed (i.e., shadow and green colored regions in the land areas may be classified as water, and waves and noises in the water areas as land).

A supervised learning-based approach that translates the land–sea segmentation problem to a binary classification task was illustrated by Wang et al. (2017) [83]. The first part of the approach involves the extraction of pixel-wise features, including local statistics, edge, texture, and structural information from training images. Then, a multi-feature classifier is trained and utilized to perform sea–land segmentation.

Different methods have been investigated by Bengoufa et al. (2021) [84] towards the identification of a reproducible shoreline extraction method. Approaches involved the assessment of both pixel-based and object-based image analysis on supervised machine learning classifiers (Support Vector Machine and Random Forest). In the context of object-based analysis. two segmentation algorithms were tested (multi-resolution image segmentation and mean shift segmentation); thus, in total, six different configurations have been applied. ArcGIS software was utilized to convert the classification results to vector format, and then a smoothing process was applied so as to remove noise. The accuracy of each approach was examined through in situ measurements (GPS survey), and the differences between the shorelines were calculated via DSAS software. The study showed that a Random Forest classifier with the multi-resolution algorithm (object-based approach) yielded better results for sandy coasts.

A similar case involving the application of an object-based image analysis approach has been applied by Abdel-Hamid et al. (2018) [85] for mapping mangroves, through the integration of both optical and SAR imagery. Different ML classifiers have been employed

(Random Forest, Support Vector Machine, and Classification and Regression Trees), with the highest accuracy to be observed from the combined use of optical and SAR data as input parameters, and the application of the RF algorithm. In situ data collected from field campaigns have been also used for both the training and the validation of the algorithms. The use of Random Forest, Logistic Regression, and naive Bayes tree machine learning algorithms, along with Landsat images for mangrove forest mapping and mapping, have been also investigated by Elmahdy et al. (2020) [86], whilst Toosi et al. (2020) [87] exploited Sentinel-2 and Worldview-2 imagery and the Random Forest algorithm for the classification land cover classes in a mangrove ecosystem.

Manaf et al. (2018) [88] proposed a hybridization of segmentation algorithms and ML techniques for object-based image analysis for shoreline extraction. During the study, 11 single and 4 ensemble learning classifiers have been evaluated. In the context of the hybridization process (the initial application of segmentation in order to lead to improved classification results), the application of the Simple Linear Iterative Clustering segmentation algorithm along with the Extra-Tree classifier yielded the best results.

Unsupervised machine learning approaches have also been investigated in the literature. Enguehard et al. (2022) [89] applied agglomerative hierarchical clustering so as to group coastal features such as topographic metrics, soil type, and vegetation indices, and to identify zones with similar characteristics. This tree-based approach computes the distance between the different observation pairs in order to cluster them into relevant groups. Alcaras et al. (2022) [90] investigated the applicability of K-Means and K-Nearest Neighbor (KNN) algorithms for land/sea discrimination. The approach is applied on the 10 m bands of Sentinel 2 satellite, on the Normalized Difference Water Index (NDWI), and on both of the above-mentioned inputs. It was found that both algorithms yielded good results, with the best ones to be provided from the mere use of the NDWI layer, while the unsupervised method also showcased a better performance in comparison with the KNN algorithm.

An unsupervised classification approach (K-Means) for the production of the mean maps of coastline states at different time instances was tested by Tzepkenlis et al. (2022) [91]. The approach was based on multispectral data (Sentinel 2 and Landsat imagery) and while exploiting specific remote sensing indices (i.e., NDWI, NDVI, etc.) as part of the process of generating yearly average water probability maps. Pradeep et al. (2022) [92] investigated coastal erosion and accretion, and shoreline changes due to climate change for a 14 year period through conventional RS and GIS techniques, whilst the generated data were used for training a machine learning model to predict the short-term coastal erosion status. A k-means clustering along with linear curve fitting was applied for the prediction of future shorelines. For the validation of the predicted values, error metrics such as Root Mean Squared Error and Mean Absolute Error were applied.

Other methods focus on edge detection and optimization procedures towards the automated coastline extraction. Paravolidakis et al. (2018) [93] provide an automated methodology that uses aerial images through image processing techniques aimed at region segmentation and edge detection. The initial step involves the application of an anisotropic diffusion algorithm, so as to reduce the noise and to enhance the edges of the image. Then, image segmentation is applied, splitting the image into two regions (land and water) using suitable thresholds that are derived from local area characteristics. As a final step, and due to the fact that objects near the coastline affect the result, an active contour method is adopted, allowing for the identification of deformations to occur using such physical objects. The processes of thresholding, edge detection, and active contour-fitting improved the accuracy of the extracted coastline.

In order to address the limitations observed by thresholding approaches that focus only on the spectral information of each image pixel without considering the neighboring ones, as well as the challenges observed in the cases of images with complex semantic information (i.e., a dependence on manually selected features and a high rate of misclas-

sified pixels), deep learning-based methodologies have been investigated for coastline monitoring applications.

Aryal et al. (2021) [94] evaluated the use of remote sensing indices, machine learning models (Random Forest and eXtreme Gradient Boosting) and a deep learning approach (a modified U-Net architecture), along with very-high-resolution spaceborne imagery for coastline mapping in the Arctic. The introduced framework is focused on a water/land semantic segmentation (pixel-wise classification) approach, being able to use sparsely labeled data for generating a dense grid of segmented labels, and thus addressing the cases of limited data availability. Despite providing good results, the deep learning-based U-Net model is slightly outperformed by single pixel models such as Random Forest. According to the authors, this might be attributed to training with sparsely labeled data, as the neural network architecture might not be able to exploit the full spatial properties of the model. In other works, the utilization of deep learning methods with an increased number of land cover classes showcased better results [108].

Aiming to identify shoreline changes, Syaifulnizam et al. (2018) [95] also utilized supervised machine learning techniques (Multilayer Perceptron Artificial Neural Network, K-Nearest Neighbor, and Support Vector Machine) for the classification of satellite images (Landsat and SPOT-5) in land and in water. Then, the boundaries of the abovementioned classes were located and properly processed (the smoothing process), so as to enable the proper extraction of the shoreline, since some issues were observed between the classification accuracy and the quality of the derived shoreline [109]. Data validation was achieved via the available reference shoreline data, whilst the Multilayer Perceptron Artificial Neural Network model was the most effective one. Finally, the GIS environment was selected for the calculation of the rate of change statistics for the available timeseries shoreline data; yet, the selection of only two classes for the classification prevents the elicitation of more fine-grained information regarding the occurrence of coastal erosion. A similar study [96] was conducted by the authors, that used pixel-based approaches to classify land–water classes using the majority voting of ensemble and single classifiers. Overall, 11 single classifiers and 4 ensemble classifiers were tested, with MLP to demonstrate the highest accuracy, whilst the combination of ensemble classifiers (Random Forest and SVM) using majority voting algorithm was proven to be the most effective method.

Building on the outputs of the previous work, Celik and Gazioglou (2022) [97] assessed the accuracy of three machine learning classifier groups (Support Vector Machines, Multilayer Perceptron (MLP), and Ensemble Learning classifiers) on different coastal types for coastline extraction. Four kernel functions and four activation functions were tested for SVM, as well as for the MLP and EL classifiers, respectively. For the evaluation, manually extracted coastlines were compared with the estimated ones in order to determine the accuracy of the classifiers in their predictions. The coastlines were broken down to segments according to their type. It was observed that the existence of shaded areas in the bedrock coasts confused the classifiers in their predictions, whilst the most accurate productions were provided by MLP with linear, logarithmic, and tanh activation functions. For beaches, MLP and SVM with linear kernel provided accurate and consistent results, whilst the rest of the methods were affected by the shallow water depths and suspended solids. Finally, for artificial coasts, the best results were seen from MLP classifiers.

Ruirui et al. [98] reviewed the relevant convolutional neural network architectures applied for sea–land segmentation problem, and introduced an improved novel deep convolutional neural network called DeepUNet. The architecture of the proposed network involves the concatenation of the layers in the contracting path, so as for sequential convolution layers to collect outputs with a higher accuracy based on the extracted data. The images used in the context of this analysis are rendered from Google Earth, covering the RGB part of the spectrum, but they are of unknown locations and resolutions. A promising overlap tiles strategy is also proposed, so as to predict the pixels in the border region of the image/tile, by assigning weights for overlap areas that are computed by the Gaussian function, considering the distance between current pixels and the center of the tile. How-

ever, it seems the accuracy of the segmentation task is not adequate for cases with smooth sea–land boundaries or complex structures.

To address such issues, Shamsolmoali et al. [99] introduced a new deep learning architecture (RDU-Net) for end-to-end pixel wise segmentation that utilizes convolution layers and multiscale densely connected residual network blocks in each layer of the network. The model was evaluated along with other traditional machine learning, as well as deep learning models (including the DeepUNet), showcasing an improved performance of its ability to extract deep features and to hierarchically reuse them to achieve accurate end-to-end image segmentation. Another deep learning-based sea–land segmentation model called Res-UNet was introduced in [100]. The approach relies on the U-Net architecture, replacing its contraction part with ResNet [110]. The network prediction labels are further post-processed through a fully connected Conditional Random Field image processing technique, whilst a morphological operation is also applied to further reduce isolated/scatter pixels in the label images.

One of the key challenges being faced by the abovementioned approaches involves the loss of boundary accuracy during the down-sampling operation of the encoder of the model, and subsequently, the lack of a reverse process (i.e., reconstruction) in the decoder, which prevents the accurate identification of the position of the water/land boundary. Aiming to improve the positional accuracy of the coastline extraction task, Jing et al. (2021) [101] proposed a multi-task network called BS-Net that adds a learning boundary coastline positioning stream to understand the exact position of the coastline, along with the segmentation network. The overall approach lies on the fusion of the water/land semantic features with the boundary features. The research work compared this approach with other thresholding methods (i.e., NDWI), machine learning models (i.e., SVM), and other deep learning architectures for semantic segmentation. The approach could lead to improved results in comparison with other methods, while also exhibiting a high consistency between the extracted water/land boundaries and the actual coastlines. Further to that, Cui et al. (2021) [102] attempted to improve the classic encoder–decoder structure and propose a deep learning model called SANet for sea–land segmentation that is based on adaptive multiscale feature learning. The approach allows for the extraction of multiscale detailed information and the contextual semantic information of objects that can subsequently and adaptively fuse feature maps of different scales.

Seale et al. (2022) [33] presented a labeled image dataset suitable for the automated extraction of coastline morphological features from Copernicus Sentinel 2 imagery. The dataset aims to address the current lack of openly available resources that prevent the benchmarking of machine learning models and cross applications comparisons and evaluation, while enabling an enhanced understanding of how model performance metrics relate to the spatial qualities of the extracted geomorphological features. The study employs different convolutional neural network models in order to detect coastline morphology and to provide a baseline performance against the dataset. It was demonstrated that the U-Net model optimized using the Sobel-edge loss function led to an improvement of image segmentation tasks for shoreline detection, in comparison to more commonly used loss functions.

Dang et al. (2022) [103] proposed a system relying on indicators that was utilized as the basis for the computation of deep learning models towards the identification of coastlines and shorelines. Considering the fact that different model structures can lead to different performances, four structures were tested, including UNet, UNet3+ (applying a connection between encoders–decoders, as well as a connection between decoders, allowing for the elicitation of detailed information and refined semantics from full scale data), U2-Net (allowing for the acquisition of deeper connections and with higher resolution, and while employing a set of encoders, a set of decoders, and a fusion module linking encoder–decoder stages) and DexiNed (facilitating the detection of end-to-end characteristics computed in shallow layers). The scope of the application of the above-mentioned models was also made in order to allow for the assessment of the rate of erosion/accretion.

The U-Net model with an image input size of 512 × 512 yielded the highest accuracy, enabling the effective identification of coastlines and shorelines towards assessing coastal erosion due to sea level rise.

A validation of Sentinel-2-based subpixel instantaneous shoreline extraction was performed by Pucino et al. (2022) [104], with data being collected from drone surveys and other in situ measurements. For the shoreline extraction, different methods were evaluated, including water indices, CoastSat [105], and a tidal-balanced convolutional neural network, whilst the approach considers each satellite image as a single point instead of image composites. The latter is applied in order to ensure the availability of an adequate number of images to support the short-term quantification of shoreline changes, and thus capture relevant seasonal events. Various CNN models have been tested, and the authors concluded with a U-Net+++ with deep supervision architecture, while also applying binary focal Jaccard as loss function and Adam optimizer. It was found that in general, neural network-based approaches provided lower accuracies in comparison to water indices, while in some cases, U-Net+++ outperformed the best water index-based approach (cases with unbalanced land and water peaks). It should be mentioned also that the U-Net+++ approach does not involve a specific threshold, rather than being self-adjusted and assigning the probability of a pixel to be classified as water, based on the contextual information available. Thus, the system should be designed and implemented in order to incorporate the various lightning and geomorphological conditions.

3.2. Results Categorization and Groupings

Research papers have been classified into four categories based on the coastline/shoreline length where the machine learning methods have been applied, including local (<20 km), regional (20–500 km), national/transnational (>500 km), and global (Figure 1). As it can be seen, the majority of the studies were conducted at local and regional scales. Additionally, 38% of the reviewed papers have been applied in Asian countries while being followed by applications in North America and Europe (21% and 18% of the reviewed papers, respectively).

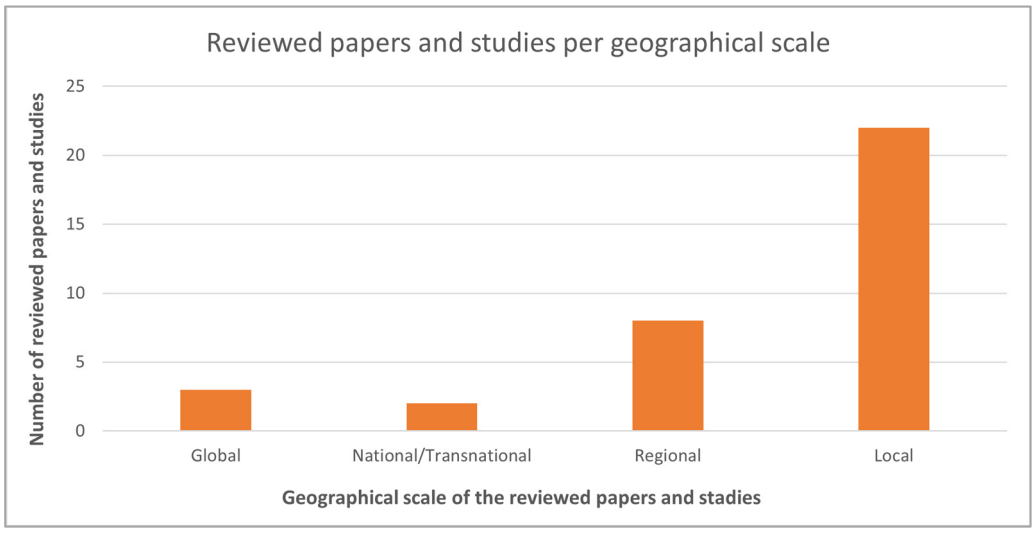

Figure 1. Categorization of reviewed papers and studies, based on their geographical scales.

Optical sensors have been widely used by the research community in the scope of coastal monitoring applications. The most widely used source of remote sensing data has been Landsat missions. Approximately half of the studies have exploited Landsat 5, 7, and 8 imageries, providing a large time series data archive. Sentinel 2 data have been also utilized, to a smaller extent (seven papers), appearing particularly during 2021 and 2022 (Figure 2). A considerable number of studies also utilized very-high-resolution data such as Google Earth composites, WorldView, RapidEye, or other aerial/satellite-based missions

for extracting information from coastal features. On the other hand, very few papers have harnessed SAR data (i.e., Sentinel 1 and ALOS/PALSAR) along with machine learning algorithms for coastline extraction.

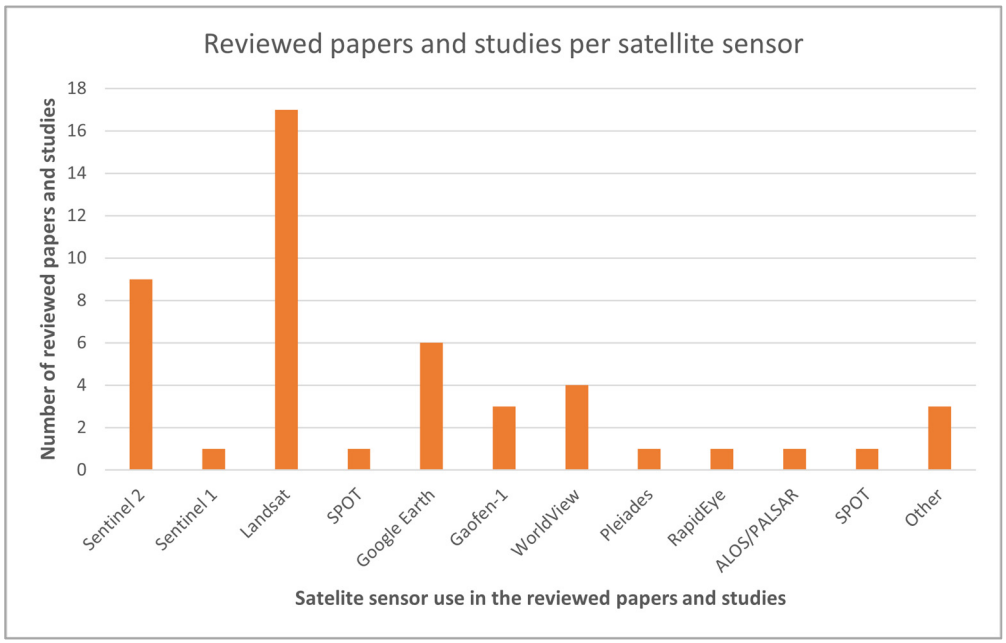

Figure 2. Categorization of reviewed papers and studies via satellite sensor.

Further to that, it can be seen that research studies investigate various machine learning techniques in the context of extracting shorelines/coastlines and the monitoring of relevant changes in the coastal environment. Approximately 25% of the studies assess the use of ensemble learning classifiers (Random Forest, Gradient Boosting, Extra Trees, and Adaptive Boosting), with the most frequently used algorithm to be the one of Random Forest. Additionally, quite a number of studies investigate the use of single machine learning classifiers such as Support Vector Machine, neural network-based approaches such as Multilayer Perceptron, and more complex deep learning architectures such as Convolutional Neural Networks (Figure 3).

When it comes to the shoreline indicators, the majority of the studies apply different machine learning techniques for the extraction of sea–land or water/dry boundaries. In some cases, the tidal data are used as part of the classification/segmentation scheme (i.e., [81,104]), whilst in other cases, the tidal data are used for subsequent corrections of errors in the retrieved shorelines (i.e., [92,105,106]). Most of the studies apply supervised machine learning techniques, and only a few cases have been identified where unsupervised methods are utilized (i.e., [74,89,91,92]. Both pixel and object-based approaches have been utilized while the problem statement can be addressed either as a classification (i.e., [63,75,79–81,90]) or a segmentation task. The latter includes cases of thresholding segmentation that take into account mainly the spectral features of the pixels (i.e., [94]) and object-based segmentation (i.e., [85]) that in some cases is followed from classification tasks in order to yield better results (i.e., [84,88]), and deep-learning concepts for semantic segmentation tasks (i.e., [99–102,110]). In many cases, the extracted shorelines are merely evaluated on the basis of the applied models' metrics (i.e., [33,76,82,94,100,107,109]), or the validation is achieved through reference shorelines that are extracted manually from satellite images (i.e., [78,83,97,99]). Only a few studies attempt to use in situ data for the validation of the models' results [81,84,85,87,93,104], while there are cases where the authors emphasize merely on the evaluation of their proposed architecture, with the results and the extracted shorelines from other/previous methods/studies (i.e., [98,99,101]).

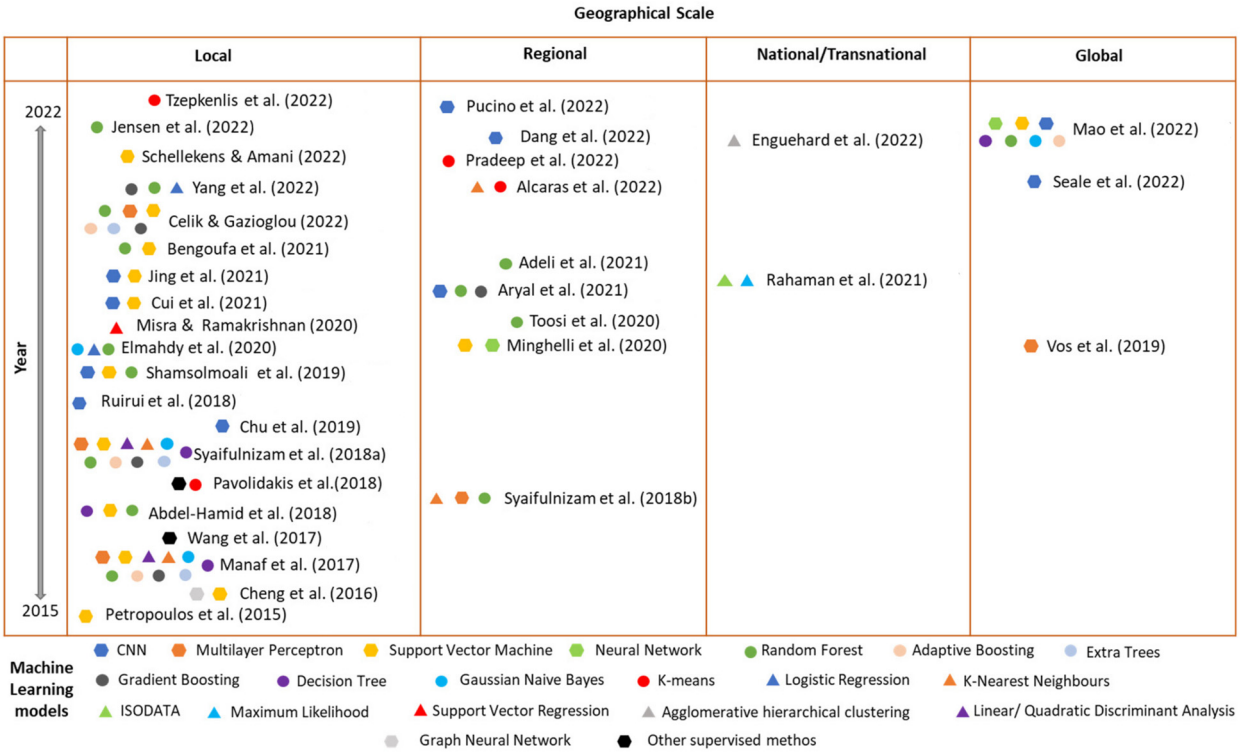

Figure 3. Schematic representation of the machine learning techniques investigated in the literature for shoreline/coastline extraction and monitoring of coastal dynamics [33,74–105,107].

4. Discussion

Coastal zones are dynamic and complex environments consisting of heterogeneous and diverse geomorphological features, while exhibiting different scales and spectral responses. Thus, the monitoring of changes in the coastal land classes and the extraction of coastlines/shorelines can be a challenging task.

Earth observation-based approaches for shoreline extraction should investigate the relationships between scene-dependent variables and shoreline accuracies, so as to better understand coast-scale performance variations. The availability and quality of other physical parameters such as waves, tides, and beach slope can influence the shoreline detection task and the accuracy of the methods.

Approaches relying on water indexes are quite common in the studies for monitoring shoreline/coastline extraction, and subsequent changes due to events. However, the use of single band images and the application of thresholding techniques can lead to controversial results when it comes to continuous monitoring applications. This is due to the fact that each new image consists of different illumination conditions, and thus requires continuous adjustments of the threshold, so as to lead to stable results. The application of normalized or standardized surface reflectance could address such issues.

Neural network-driven approaches should take into account and be trained so as to discriminate between water and land at different tidal phases. Additionally, studies have shown that increasing the input size of the machine learning model could lead to more spatial and attribute details about coastline/shorelines, facilitating land–water discrimination, as well as the detection of space between them. Moreover, recent studies employing more complex architectures (i.e., neural networks) mainly exploit RGB bands. The use of additional spectral bands could also be useful in obtaining different results, whilst the use of indexes (i.e., NDWI) apart from the spectral bands can lead to improved model results.

In cases where object-based analysis is used as the basis of coastal classification, different segmentation approaches could provide different classification results. It seems

also that pixel-based approaches are more sensitive to coastline characteristics and heterogeneities (i.e., dunes, vegetation, etc.) compared to object-based approaches, in which apart from spectral information, other properties (i.e., shape, texture, etc.) can be considered as well. However, in the context of object-based segmentation approaches, it might be difficult to select the appropriate scale when it comes to large-scale studies, and thus, subsequent steps such as classification might be required.

Deep learning introduces new innovative concepts for semantic segmentation and classification tasks. Deep learning architectures have good generalization and could support different scenarios of land/water segmentation towards the extraction of shorelines. Current research trends emphasize on addressing cases of complex shorelines in terms of their sizes, shapes, and compositions.

Differences in the reflectances of the different coastal elements can facilitate the extraction of coastlines. However, the existence of shaded/unshaded areas can lead to discrepancies in the characterization. The existence of clouds (particularly in the countries of the northern hemisphere) could further hinder characterization. The combination of approaches relying both on optical and SAR data could be useful in addressing such cases.

Very-high-resolution data can also lead to more accurate results in the shoreline extraction process. However, these data are usually costly and thus cannot be easily applied for large-scale monitoring. Future works should emphasize on multi-modal data fusion, so as to improve the spatial and spectral details of the objects that impact on the shoreline extraction task.

The validation of shoreline/coastline positions is also of paramount importance, yet very few studies [81,84,85,93,104] quantify positional errors through other in situ data. The widespread availability of in situ data can facilitate the development of new machine learning models, as well as the calibration and validation of algorithms by the research community.

In the context of cases that need to investigate coastal erosion due to climate change, sea level rise, or other phenomena, the monitoring of coastlines is more appropriate, whilst shorelines seem to be more suitable for monitoring tidal-datum indicators.

Last but not least, it should be stated that machine learning techniques have been also applied to the coastal environment in the context of other application focuses, such as the monitoring of marine litter and the extraction of wave and tide parameters from multimedia (i.e., videos). Litter classification tasks can be achieved by applying similar approaches with the ones investigated in this paper [111], whilst typical examples of the latter require different convolutional neural network architectures, in which each tide class is classified to a tide height in each video frame, and optical flow techniques can be applied for the calculation of waves flows and heights [30].

5. Conclusions

In the context of this study, 36 papers were selected and analyzed, covering different cases of coastline/shoreline extraction and change analysis, and/or coastal dynamic monitoring through the use of machine learning. Particular emphasis was given on the different machine learning approaches applied by the research community in conjunction with the Earth Observation data, used as well as the problem statement. The overall remark of this study is that there is no standardized approach that could be applied for the extraction of shorelines and the monitoring of relevant phenomena (i.e., coastal erosion), considering the complexity and heterogeneity of the coastal environments, and particularly the sizes, shapes, and compositions of the shorelines, as well as the scale of the phenomenon under investigation. The use of neural networks and deep learning approaches is expected to further increase in the coming years, given their ability to provide a good generalization and to support different scenarios of land/water segmentation and coastal classification.

Author Contributions: Conceptualization, C.-A.D.T. and C.C.; methodology, C.C.; software, C.-A.D.T.; validation, C.-A.D.T. and C.C.; formal analysis, C.-A.D.T. and C.C.; investigation, C.-A.D.T.; resources, C.C.; data curation, C.-A.D.T.; writing—original draft preparation, C.-A.D.T.; writing—review and editing, C.C.; visualization, C.-A.D.T.; supervision, C.C.; project administration, C.-A.D.T. and C.C. All authors have read and agreed to the published version of the manuscript.

Funding: This research received no external funding.

Institutional Review Board Statement: Not applicable.

Informed Consent Statement: Not applicable.

Data Availability Statement: Not applicable.

Conflicts of Interest: The authors declare no conflict of interest.

References

1. Neumann, B.; Ott, K.; Kenchington, R. Strong sustainability in coastal areas: A conceptual interpretation of SDG 14. *Sustain. Sci.* **2017**, *12*, 1019–1035. [CrossRef]
2. Le Cozannet, G.; Bulteau, T.; Castelle, B.; Ranasinghe, R.; Wöppelmann, G.; Rohmer, J.; Bernon, N.; Idier, D.; Louisor, J.; Salasy-Mélia, D. Quantifying uncertainties of sandy shoreline change projections as sea level rises. *Sci. Rep.* **2019**, *9*, 42. [CrossRef]
3. Athanasiou, P.; van Dongeren, A.; Giardino, A.; Vousdoukas, M.I.; Ranasinghe, R.; Kwadijk, J. Uncertainties in projections of sandy beach erosion due to sea level rise: An analysis at the European scale. *Sci. Rep.* **2020**, *10*, 11895. [CrossRef] [PubMed]
4. Boak, E.H.; Turner, I.L. Shoreline Definition and Detection: A Review. *J. Coast. Res.* **2005**, *214*, 688–703. [CrossRef]
5. Ankrah, J.; Monteiro, A.; Madureira, H. Bibliometric Analysis of Data Sources and Tools for Shoreline Change Analysis and Detection. *Sustainability* **2022**, *14*, 4895. [CrossRef]
6. Pajak, M.J.; Leatherman, S. The high-water line as shoreline indicator. *J. Coast. Res.* **2002**, *18*, 329–337.
7. Zhang, K.; Douglas, B.C.; Leatherman, S.P. Global Warming and Coastal Erosion. *Clim. Chang.* **2004**, *64*, 41–58. [CrossRef]
8. Robertson, W.; Whitman, D.; Zhang, Z.; Leatherman, S.P. Mapping Shoreline Position Using Airborne Laser Altimetry. *J. Coast. Res.* **2004**, *20*, 884–892. Available online: http://www.jstor.org/stable/4299347 (accessed on 10 January 2023). [CrossRef]
9. Sekovski, I.; Stec, F.; Mancini, F.; Del Rio, L. Image classification methods applied to shoreline extraction on very high-resolution multispectral imagery. *Int. J. Remote Sens.* **2014**, *35*, 3556–3578. [CrossRef]
10. Guariglia, A.; Buonamassa, A.; Losurdo, A.; Saladino, R.; Trivigno, M.L.; Zaccagnino, A.; Colangelo, A. A Multisource Approach for Coastline Mapping and Identification of Shoreline Changes. *Ann. Geophys.* **2006**, *41*, 295–304. [CrossRef]
11. Ruiz, L.A.; Pardo, J.E.; Almonacid, J.; RodríGuez, B. Coastline Automated Detection and Multiresolution Evaluation Using Satellite Images. In Proceedings of the Coastal Zone 07, Portland, OR, USA, 22–26 July 2007.
12. Sunder, S.; Ramsankaran, R.; Ramakrishnan, B. Inter-comparison of remote sensing sensing-based shoreline mapping techniques at different coastal stretches of India. *Environ. Monit. Assess.* **2017**, *189*, 290. [CrossRef] [PubMed]
13. Young, A.P.; Guza, R.T.; Dickson, M.E.; O'Reilly, W.C.; Flick, R.E. Ground motions on rocky, cliffed, and sandy shorelines generated by ocean waves. *J. Geophys. Res. Oceans* **2013**, *18*, 2169–9275. [CrossRef]
14. Young, A.P.; Guza, R.T.; Dickson, M.E.; O'Reilly, W.C.; Flick, R.E. Observations of coastal cliff base waves, sand levels, and cliff top shaking. *Earth Surf. Process. Landf.* **2016**, *41*, 1564–1573. [CrossRef]
15. Eguchi, B.M.M.; Albino, J. Bluff retreat induced by wave action on a tropical beach, in Espírito Santo, Brazil. *Rev. Bras. Geofis.* **2018**, *36*, 569–580. [CrossRef]
16. Stockdon, H.F.; Doran, K.S.; Sallenger, A.H. Extraction of lidar based dune crest elevations for use in examining the vulnerability of beaches to inundation during hurricanes. *J. Coast. Res.* **2009**, *25*, 59–65. [CrossRef]
17. Wernette, P.; Houser, C.; Bishop, M.P. An automated approach for extracting Barrier Island morphology from digital elevation models. *Geomorphology* **2016**, *262*, 1–7. [CrossRef]
18. Merlotto, A.; B'ertola, G.R.; Isla, F.I.; Cortizo, L.C.; Piccolo, M.C. Short and medium-term coastal evolution of Necochea municipality, Buenos Aires province, Argentina. *Environ. Earth Sci.* **2014**, *71*, 1213–1225. [CrossRef]
19. Pye, K.; Blot, S.J. Assessment of beach and dune erosion and accretion using lidar: Impact of the stormy 2013–14 winter and longer term trends on the Sefton Coast, UK. *Geomorphology* **2016**, *266*, 146–167. [CrossRef]
20. Scaioni, M.; Longoni, L.; Melillo, V.; Papini, M. Remote sensing for landslide investigations: An overview of recent achievements and perspectives. *Remote Sens.* **2014**, *6*, 9600–9652. [CrossRef]
21. Balaji, R.; Sathish Kumar, S.; Misra, A. Understanding the effects of seawall construction using a combination of analytical modelling and remote sensing techniques: Case study of Fansa, Gujarat, India. *Int. J. Ocean Clim. Syst.* **2017**, *8*, 153–160. [CrossRef]
22. Ferreira, O.; Garcia, T.; Matias, A.; Tabordac, R.; Dias, J.A. An Integrated Method For The Determination Of Set-Back Lines For Coastal Erosion Hazards On Sandy Shores. *Cont. Shelf Res.* **2006**, *26*, 1030–1044. [CrossRef]
23. Lira, C.; Taborda, R. Advances in applied remote sensing to coastal environments using free satellite imagery. *Coast. Res. Libr.* **2014**, *9*, 77–102. [CrossRef]

24. Cenci, L.; Disperati, L.; Persichillo, M.G.; Oliveira, E.R.; Alves, F.L.; Phillips, M. Integrating remote sensing and GIS techniques for monitoring and modeling shoreline evolution to support coastal risk management. *GIScience Remote Sens.* **2018**, *55*, 355–375. [CrossRef]
25. Ahsanullah; Shaukat, H.K.; Razzaq, A.; Muhammad, L. Morphological change detection along the shoreline of Karachi, Pakistan using 50 year time series satellite remote sensing data and GIS techniques. *Geomat. Nat. Hazards Risk* **2021**, *12*, 3358–3380. [CrossRef]
26. Liu, H.; Sherman, D.; Gu, G. Automated extraction of shorelines from airborne light detection and ranging data and accuracy assessment based on Monte Carlo simulation. *J. Coast. Res.* **2007**, *23*, 1359–1369. Available online: https://www.jstor.org/stable/30138535 (accessed on 10 January 2023). [CrossRef]
27. Miller, J.K.; Dean, R.G. Shoreline variability via empirical orthogonal function analysis: Part I temporal and spatial characteristics. *Coast. Eng.* **2007**, *54*, 111–131. [CrossRef]
28. Reeve, D.E.; Spivack, M. Evolution of shoreline position moments. *Coast. Eng.* **2004**, *51*, 661–673. [CrossRef]
29. Aagaard, T.; Davidson-Arnott, R.; Greenwood, B.; Nielsen, J. Sediment Supply from Shoreface to Dunes: Linking Sediment Transport Measurements and Long-Term Morphological Evolution. *Geomorphology* **2004**, *60*, 205–224. [CrossRef]
30. Scardino, G.; Scicchitano, G.; Chirivì, M.; Costa, P.J.M.; Luparelli, A.; Mastronuzzi, G. Convolutional Neural Network and Optical Flow for the Assessment of Wave and Tide Parameters from Video Analysis (LEUCOTEA): An Innovative Tool for Coastal Monitoring. *Remote Sens.* **2022**, *14*, 2994. [CrossRef]
31. Thieler, E.R.; Himmelstoss, E.A.; Zichichi, J.L.; Ergul, A. *Digital Shoreline Analysis System (DSAS) Version 4.0—An ArcGIS Extension for Calculating Shoreline Change*; U.S. Geological Survey: Reston, VA, USA, 2009; ISBN 2008-1278. [CrossRef]
32. Gómez-Pazo, A.; Payo, A.; Paz-Delgado, M.V.; Delgadillo-Calzadilla, M.A. Open Digital Shoreline Analysis System: ODSAS v1.0. *J. Mar. Sci. Eng.* **2022**, *10*, 26. [CrossRef]
33. Seale, C.; Redfern, T.; Chatfield, P.; Luo, C.; Dempsey, K. Coastline detection in satellite imagery: A deep learning approach on new benchmark data. *Remote Sens. Environ.* **2022**, *278*, 113044. [CrossRef]
34. McAllister, E.; Payo, A.; Novellino, A.; Dolphin, T.; Medina-Lopez, E. Multispectral satellite imagery and machine learning for the extraction of shoreline indicators. *Coast. Eng.* **2022**, *174*, 104102. [CrossRef]
35. Gagliardi, V.; Tosti, F.; Bianchini Ciampoli, L.; Battagliere, M.L.; D'Amato, L.; Alani, A.M.; Benedetto, A. Satellite Remote Sensing and Non-Destructive Testing Methods for Transport Infrastructure Monitoring: Advances, Challenges and Perspectives. *Remote Sens.* **2023**, *15*, 418. [CrossRef]
36. Ustin, S.L.; Middleton, E.M. Current and near-term advances in Earth observation for ecological applications. *Ecol. Process.* **2021**, *10*, 1. [CrossRef]
37. Paz-Delgado, M.V.; Payo, A.; Gómez-Pazo, A.; Beck, A.-L.; Savastano, S. Shoreline Change from Optical and Sar Satellite Imagery at Macro-Tidal Estuarine, Cliffed Open-Coast and Gravel Pocket-Beach Environments. *J. Mar. Sci. Eng.* **2022**, *10*, 561. [CrossRef]
38. Teodoro, A.C. Optical satellite remote sensing of the coastal zone environment: An overview. In *Environmental Applications of Remote Sensing*; Marghany, M., Ed.; IntechOpen: London, UK, 2016; pp. 165–196. [CrossRef]
39. Buono, A.; Ferrentino, E.; Li, Y.; de Macedo, C.R. Ocean and Coastal Area Information Retrieval Using SAR Polarimetry. In *Springer Optimization and Its Applications*; Rysz, M., Tsokas, A., Dipple, K.M., Fair, K.L., Pardalos, P.M., Eds.; Synthetic Aperture Radar (SAR) Data Applications; Springer: Cham, Switzerland, 2022; Volume 199. [CrossRef]
40. Yang, X.; Zhao, J.; Wei, Z.; Wang, N.; Gao, X. SAR-to-optical image translation based on improved CGAN. *Pattern Recognit.* **2022**, *121*, 108208. [CrossRef]
41. Jutz, S.; Milagro-Pérez, M. Copernicus: The European Earth Observation Programme. *Rev. Teledetec.* **2020**, *56*, 5–11. [CrossRef]
42. Masson-Delmotte, V.; Zhai, P.; Pirani, A.; Connors, S.L.; Péan, C.; Berger, S.; Caud, N.; Chen, Y.; Goldfarb, L.; Gomis, M.I.; et al. *IPCC, 2021: Climate Change 2021: The Physical Science Basis. Contribution of Working Group I to the Sixth Assessment Report of the Intergovernmental Panel on Climate Change*; Cambridge University Press: Cambridge, UK; New York, NY, USA, 2021; *In press*. [CrossRef]
43. Phiri, D.; Simwanda, M.; Salekin, S.; Nyirenda, V.R.; Murayama, Y.; Ranagalage, M. Sentinel-2 Data for Land Cover/Use Mapping: A Review. *Remote Sens.* **2020**, *12*, 2291. [CrossRef]
44. Vreugdenhil, M.; Navacchi, C.; Bauer-Marschallinger, B.; Hahn, S.; Steele-Dunne, S.; Pfeil, I.; Dorigo, W.; Wagner, W. Sentinel-1 Cross Ratio and Vegetation Optical Depth: A Comparison over Europe. *Remote Sens.* **2020**, *12*, 3404. [CrossRef]
45. Almonacid-Caballer, J.; Sánchez-García, E.; Pardo-Pascual, J.; Balaguer-Beser, A.; Palomar-Vázquez, J. Evaluation of annual mean shoreline position deduced from Landsat imagery as a mid-term coastal evolution indicator. *Mar. Geol.* **2016**, *372*, 79–88. [CrossRef]
46. James, D.; Collin, A.; Mury, A.; Qin, R. Satellite–Derived Topography and Morphometry for VHR Coastal Habitat Mapping: The Pleiades–1 Tri–Stereo Enhancement. *Remote Sens.* **2022**, *14*, 219. [CrossRef]
47. Loghin, A.-M.; Otepka-Schremmer, J.; Pfeifer, N. Potential of Pléiades and WorldView-3 Tri-Stereo DSMs to Represent Heights of Small Isolated Objects. *Sensors* **2020**, *20*, 2695. [CrossRef] [PubMed]
48. Turner, I.; Harley, M.; Almar, R.; Bergsma, E. Satellite optical imagery in Coastal Engineering. *Coast. Eng.* **2021**, *167*, 103919. [CrossRef]
49. Bartsch, A.; Ley, S.; Nitze, I.; Pointner, G.; Vieira, G. Feasibility Study for the Application of Synthetic Aperture Radar for Coastal Erosion Rate Quantification Across the Arctic. *Front. Environ. Sci.* **2020**, *8*, 143. [CrossRef]

50. Fischer, P.; Dietrich, P.; Achterberg, E.; Anselm, N.; Brix, H.; Bussmann, I.; Eickelmann, L.; Flöser, G.; Friedrich, M.; Rust, H.; et al. Effects of Measuring Devices and Sampling Strategies on the Interpretation of Monitoring Data for Long-Term Trend Analysis. *Front. Mar. Sci.* **2021**, *8*, 770977. [CrossRef]
51. Arabi, B.; Salama, M.S.; Pitarch, J.; Verhoef, W. Integration of In-Situ and Multi-Sensor Satellite Observations for Long-Term Water Quality Monitoring in Coastal Areas. *Remote Sens. Environ.* **2020**, *239*, 111632. [CrossRef]
52. Dong, J.; Hao, M.; Fu, J. *Monitoring the Coastal Environment Using Remote Sensing and GIS Techniques*; IntechOpen: London, UK, 2016; Available online: https://www.intechopen.com/chapters/49930 (accessed on 10 January 2023).
53. Elmes, A.; Alemohammad, H.; Avery, R.; Caylor, K.; Eastman, J.R.; Fishgold, L.; Friedl, M.A.; Jain, M.; Kohli, D.; Laso Bayas, J.C.; et al. Accounting for Training Data Error in Machine Learning Applied to Earth Observations. *Remote Sens.* **2020**, *12*, 1034. [CrossRef]
54. Hauser, L.T.; Féret, J.-B.; Binh, N.A.; Windt, N.v.d.; Sil, Â.F.; Timmermans, J.; Soudzilovskaia, N.A.; van Bodegom, P.M. Towards Scalable Estimation of Plant Functional Diversity from Sentinel-2: In-situ Validation in a Heterogeneous (Semi-) Natural Landscape. *Remote Sens. Environ.* **2021**, *262*, 112505. [CrossRef]
55. Wei, M.L. *Python Machine Learning*, 5th ed.; John Wiley & Sons, Inc.: Hoboken, NJ, USA, 2019.
56. Zhang, Y. *New Advances in Machine Learning*; Intech Open: London, UK, 2010; ISBN 978-953-307-034-6. [CrossRef]
57. Ferreira, B.; Silva, R.G.; Iten, M. Earth Observation Satellite Imagery Information Based Decision Support Using Machine Learning. *Remote Sens.* **2022**, *14*, 3776. [CrossRef]
58. Taeho, J. *Machine Learning Foundations Supervised, Unsupervised, and Advanced Learning*; Springer Nature: Cham, Switzerland, 2021. [CrossRef]
59. Ho, T.K. Random Decision Forests. In Proceedings of the 3rd International Conference on Document Analysis and Recognition, Montreal, QC, Canada, 14–16 August 1995; pp. 278–282. [CrossRef]
60. Foody, G.M.; Mathur, A. Toward intelligent training of supervised image classifications: Directing training data acquisition for SVM classification. *Remote Sens. Environ.* **2004**, *93*, 107–117. [CrossRef]
61. Bai, B.; Tan, Y.; Donchyts, G.; Haag, A.; Xu, B.; Chen, G.; Weerts, A. Naive Bayes classification-based surface water gap-filling from partially contaminated optical remote sensing image. *J. Hydrol.* **2023**, *616*, 128791. [CrossRef]
62. Liu, K.; Li, X.; Shi, X.; Wang, S. Monitoring mangrove forest changes using remote sensing and GIS data with decision-tree learning. *Wetlands* **2008**, *28*, 336–346. [CrossRef]
63. Russell, S.; Norvig, P. *Artificial Intelligence: A Modern Approach*, 2nd ed.; Prentice Hall: Hoboken, NJ, USA, 2003; ISBN 978-0137903955.
64. Cover, T.M.; Hart, P.E. Nearest neighbor pattern classification. *IEEE Trans. Inf. Theory* **1967**, *13*, 21–27. [CrossRef]
65. Abdul Gafoor, F.; Al-Shehhi, M.R.; Cho, C.-S.; Ghedira, H. Gradient Boosting and Linear Regression for Estimating Coastal Bathymetry Based on Sentinel-2 Images. *Remote Sens.* **2022**, *14*, 5037. [CrossRef]
66. Kim, S.-J.; Bae, S.-J.; Jang, M.-W. Linear Regression Machine Learning Algorithms for Estimating Reference Evapotranspiration Using Limited Climate Data. *Sustainability* **2022**, *14*, 11674. [CrossRef]
67. Goodfellow, H.; Bengio, Y.; Courville, A. Deep learning. *Genet. Program. Evolvable Mach.* **2018**, *19*, 305–307. [CrossRef]
68. Ding, Z.; Su, F.; Zhang, J.; Zhang, Y.; Luo, S.; Tang, X. Clustering Coastal Land Use Sequence Patterns along the Sea–Land Direction: A Case Study in the Coastal Zone of Bohai Bay and the Yellow River Delta, China. *Remote Sens.* **2019**, *11*, 2024. [CrossRef]
69. Wattelez, G.; Dupouy, C.; Juillot, F. Unsupervised Optical Classification of the Seabed Color in Shallow Oligotrophic Waters from Sentinel-2 Images: A Case Study in the Voh-Koné-Pouembout Lagoon (New Caledonia). *Remote Sens.* **2022**, *14*, 836. [CrossRef]
70. Shenbagaraj, N.; Mani, N.D.; Muthukumar, M. Isodata Classification Technique to Assess the Shoreline Changes of Kolachel to Kayalpattanam Coast. *Int. J. Eng. Res. Technol. (IJERT)* **2014**, *3*, 4.
71. Narumalani, S.; Mishra, D.; Burkholder, J.; Merani, P.; Willson, G. A Comparative Evaluation of ISODATA and Spectral Angle Mapping for the Detection of Saltcedar Using Airborne Hyperspectral Imagery. *Geocarto Int.* **2006**, *21*, 59–66. [CrossRef]
72. Wang, J.; Ding, C.H.Q.; Chen, S.; He, C.; Luo, B. Semi-Supervised Remote Sensing Image Semantic Segmentation via Consistency Regularization and Average Update of Pseudo-Label. *Remote Sens.* **2020**, *12*, 3603. [CrossRef]
73. Reddy, P.; Viswanath, P.; Reddy, B.E. Semi-Supervised Learning: A Brief Review. *Int. J. Eng. Technol.* **2018**, *7*, 81. [CrossRef]
74. Rahaman, M.; Esraz-Ul-Zannat, M. Evaluating the impacts of major cyclonic catastrophes in coastal Bangladesh using geospatial techniques. *SN Appl. Sci.* **2021**, *3*, 727. [CrossRef]
75. Yang, M.; Zou, L.; Cai, H.; Qiang, Y.; Lin, B.; Zhou, B.; Abedin, J.; Mandal, D. Spatial–Temporal Land Loss Modeling and Simulation in a Vulnerable Coast: A Case Study in Coastal Louisiana. *Remote Sens.* **2022**, *14*, 896. [CrossRef]
76. Jensen, D.J.; Cavanaugh, K.C.; Thompson, D.R.; Fagherazzi, S.; Cortese, L.; Simard, M. Leveraging the historical Landsat catalog for a remote sensing model of wetland accretion in coastal Louisiana. *J. Geophys. Res. Biogeosci.* **2022**, *127*, e2022JG006794. [CrossRef]
77. Petropoulos, G.P.; Kalivas, D.P.; Griffiths, H.M.; Dimou, P.P. Remote sensing and gis analysis for mapping spatio-temporal changes of erosion and deposition of two mediterranean river deltas: The case of the axios and aliakmonas rivers, Greece. *Int. J. Appl. Earth Obs. Geoinf.* **2015**, *35*, 217–228. [CrossRef]
78. Schellekens, J.; Amani, M. Coastal erosion detection using landsat satellite imagery and support vector machine algorithm. *J. Ocean. Technol.* **2022**, *17*, 54–64.

79. Minghelli, A.; Spagnoli, J.; Lei, M.; Chami, M.; Charmasson, S. Shoreline Extraction from WorldView2 Satellite Data in the Presence of Foam Pixels Using Multispectral Classification Method. *Remote Sens.* **2020**, *12*, 2664. [CrossRef]
80. Misra, A.; Ramakrishnan, B. Assessment of coastal geomorphological changes using multi-temporal Satellite-Derived Bathymetry. *Cont. Shelf Res.* **2020**, *207*, 104213. [CrossRef]
81. Mao, Y.; Harris, D.L.; Xie, Z.; Phinn, S. Global coastal geomorphology—Integrating earth observation and geospatial data. *Remote Sens. Environ.* **2022**, *278*, 113082. [CrossRef]
82. Cheng, D.; Meng, G.; Xiang, S.; Pan, C. Efficient sea-land segmentation using seeds learning and edge directed graph cut. *Neurocomputing* **2016**, *207*, 36–47. [CrossRef]
83. Wang, D.; Cui, X.; Xie, F.; Jiang, Z.; Shi, Z. Multi-feature sea–land segmentation based on pixel-wise learning for optical remote-sensing imagery. *Int. J. Remote Sens.* **2017**, *38*, 4327–4347. [CrossRef]
84. Bengoufa, S.; Niculescu, S.; Mihoubi, M.K.; Belkessa, R.; Rami, A.; Rabehi, W.; Abbad, K. Machine learning and shoreline monitoring using optical satellite images: Case study of the Mostaganem shoreline, Algeria. *J. Appl. Remote Sens.* **2021**, *15*, 026509. [CrossRef]
85. Abdel-Hamid, A.; Dubovyk, O.; Abou El-Magd, I.; Menz, G. Mapping Mangroves Extents on the Red Sea Coastline in Egypt using Polarimetric SAR and High Resolution Optical Remote Sensing Data. *Sustainability* **2018**, *10*, 646. [CrossRef]
86. Elmahdy, S.I.; Ali, T.A.; Mohamed, M.M.; Howari, F.M.; Abouleish, M.; Simonet, D. Spatiotemporal Mapping and Monitoring of Mangrove Forests Changes From 1990 to 2019 in the Northern Emirates, UAE Using Random Forest, Kernel Logistic Regression and Naive Bayes Tree Models. *Front. Environ. Sci.* **2020**, *8*, 102. [CrossRef]
87. Toosi, N.B.; Soffianian, A.R.; Fakheran, S.; Pourmanafi, S.; Ginzler, C.; Waser, L.T. Land cover classification in Mangrove ecosystems based on VHR satellite data and machine learning-An upscaling approach. *Remote Sens.* **2020**, *12*, 2684. [CrossRef]
88. Manaf, S.A.; Mustapha, N.; Sulaiman, N.M.; Husin, N.A.; Shafri, H.Z.M.; Razali, M.N. Hybridization of SLIC and Extra Tree for Object Based Image Analysis in Extracting Shoreline from Medium Resolution Satellite Images. *Int. J. Intell. Eng. Syst.* **2018**, *11*, 62–72. [CrossRef]
89. Enguehard, L.; Falco, N.; Schmutz, M.; Newcomer, M.E.; Ladau, J.; Brown, J.B.; Bourgeau-Chavez, L.; Wainwright, H.M. Machine-Learning Functional Zonation Approach for Characterizing Terrestrial–Aquatic Interfaces: Application to Lake Erie. *Remote Sens.* **2022**, *14*, 3285. [CrossRef]
90. Alcaras, E.; Amoroso, P.P.; Figliomeni, F.G.; Parente, C.; Vallario, A. Machine Learning Approaches for Coastline Extraction from Sentinel-2 Images: K-Means and K-Nearest Neighbour Algorithms in Comparison. In Proceedings of the 25th Italian Conference on Geomatics and Geospatial Technologies ASITA 2022, Genova, Italy, 20–24 June 2022. [CrossRef]
91. Tzepkenlis, A.; Grammalidis, N.; Kontopoulos, C.; Charalampopoulou, V.; Kitsiou, D.; Pataki, Z.; Patera, A.; Nitis, T. An Integrated Monitoring System for Coastal and Riparian Areas Based on Remote Sensing and Machine Learning. *J. Mar. Sci. Eng.* **2022**, *10*, 1322. [CrossRef]
92. Pradeep, J.; Shaji, E.; Subeesh Chandran, C.S.; Ajas, H.; Chandra, S.V.; Dev, S.D.; Babu, D.S. Assessment of coastal variations due to climate change using remote sensing and machine learning techniques: A case study from west coast of India. *Estuar. Coast. Shelf Sci.* **2022**, *275*, 107968. [CrossRef]
93. Paravolidakis, V.; Ragia, L.; Moirogiorgou, K.; Zervakis, M.E. Automatic Coastline Extraction Using Edge Detection and Optimization Procedures. *Geosciences* **2018**, *8*, 407. [CrossRef]
94. Aryal, B.; Escarzaga, S.M.; Vargas Zesati, S.A.; Velez-Reyes, M.; Fuentes, O.; Tweedie, C. Semi-Automated Semantic Segmentation of Arctic Shorelines Using Very High-Resolution Airborne Imagery, Spectral Indices and Weakly Supervised Machine Learning Approaches. *Remote Sens.* **2021**, *13*, 4572. [CrossRef]
95. Syaifulnizam, A.M.; Norwati, M.; Md Nasir, S.; Nor Azura, H.; Mohd, R.; Abdul, H. Change analysis on historical shorelines extracted from medium resolution satellite images: A case study on the southern coast of Peninsular Malaysia. In Proceedings of the 9th IGRSM International Conference and Exhibition on Geospatial & Remote Sensing (IGRSM 2018), Kuala Lumpur, Malaysia, 24–25 April 2018. [CrossRef]
96. Syaifulnizam, A.M.; Norwati, M.; Sulaiman, N.; Husin, N.A.; Zainuddin, M.N.; Shafri, H.Z. Majority voting of ensemble classifiers to improve shoreline extraction of medium resolution satellite images. *J. Theor. Appl. Inf. Technol.* **2017**, *95*, 4394–4405. Available online: http://www.jatit.org/volumes/Vol95No18/7Vol95No18.pdf (accessed on 8 January 2023).
97. Çelik, O.İ.; Gazioğlu, C. Coast type-based accuracy assessment for coastline extraction from satellite image with machine learning classifiers. *Egypt. J. Remote Sens. Space Sci.* **2022**, *25*, 289–299. [CrossRef]
98. Ruirui, L.; Wenjie, L.; Lei, Y.; Shihao, S.; Wei, H.; Fan, Z.; Wei, L. DeepUNet: A Deep Fully Convolutional Network for Pixel-Level Sea-Land Segmentation. *IEEE J. Sel. Top. Appl. Earth Obs. Remote Sens.* **2018**, *11*, 3954–3962. [CrossRef]
99. Shamsolmoali, P.; Zareapoor, M.; Wang, R.; Zhou, H.; Yang, J. A Novel Deep Structure U-Net for Sea-Land Segmentation in Remote Sensing Images. *IEEE J. Sel. Top. Appl. Earth Obs. Remote Sens.* **2019**, *12*, 3219–3232. [CrossRef]
100. Chu, Z.; Tian, T.; Feng, R.; Wang, L. Sea-land Segmentation with Res-UNet and fully connected CRF. In Proceedings of the IEEE International Geoscience and Remote Sensing Symposium, Yokohama, Japan, 28 July–2 August 2019. [CrossRef]
101. Jing, W.; Cui, B.; Lu, Y.; Huang, L. BS-Net: Using Joint-Learning Boundary and Segmentation Network for Coastline Extraction from Remote Sensing Images. *Remote Sens. Lett.* **2021**, *12*, 1260–1268. [CrossRef]
102. Cui, B.; Jing, W.; Huang, L.; Li, Z.; Lu, Y. SANet: A Sea-Land Segmentation Network Via Adaptive Multiscale Feature Learning. *IEEE J. Sel. Top. Appl. Earth Obs. Remote Sens.* **2021**, *14*, 116–126. [CrossRef]

103. Dang, K.B.; Dang, V.B.; Ngo, V.L.; Vu, K.C.; Nguyen, H.; Nguyen, D.A.; Nguyen, T.D.L.; Pham, T.P.N.; Giang, T.L.; Nguyen, H.D.; et al. Application of deep learning models to detect coastlines and shorelines. *J. Environ. Manag.* **2022**, *320*, 115732. [CrossRef]
104. Pucino, N.; Kennedy, D.M.; Young, M.; Ierodiaconou, D. Assessing the accuracy of Sentinel-2 instantaneous subpixel shorelines using synchronous UAV ground truth surveys. *Remote Sens. Environ.* **2022**, *282*, 113293. [CrossRef]
105. Vos, K.; Splinter, K.D.; Harley, M.D.; Simmons, J.A.; Turner, I.L. CoastSat: A Google Earth Engine-enabled Python toolkit to extract shorelines from publicly available satellite imagery. *Environ. Model. Softw.* **2019**, *122*, 104528. [CrossRef]
106. Tsai, Y.-L.S. Monitoring 23-year of shoreline changes of the Zengwun Estuary in Southern Taiwan using time-series Landsat data and edge detection techniques. *Sci. Total Environ.* **2022**, *839*, 156310. [CrossRef] [PubMed]
107. Adeli, S.; Salehi, B.; Mahdianpari, M.; Quackenbush, L.J.; Chapman, B. Moving toward L-Band NASA-ISRO SAR Mission (NISAR) Dense Time Series: Multipolarization Object-Based Classification of Wetlands Using Two Machine Learning Algorithms. *Earth Space Sci.* **2021**, *8*, e2021EA001742. [CrossRef]
108. Hu, Y.; Zhang, Q.; Zhang, Y.; Yan, H. A Deep Convolution Neural Network Method for Land Cover Mapping: A Case Study of Qinhuangdao, China. *Remote Sens.* **2018**, *10*, 2053. [CrossRef]
109. Syaifulnizam, A.M.; Norwati, M.; Sulaiman, N.; Husin, N.A.; Shafri, H.Z.; Hamid, M.R. Quantitative Validation Assessment on Shorelines Extracted from Image Classification Techniques of Medium Resolution Satellite Images Based on Change Analysis. *J. Telecommun. Electron. Comput. Eng.* **2017**, *9*, 67–73.
110. Kaiming, H.; Xiangyu, Z.; Shaoqing, R.; Jian, S. Deep residual learning for image recognition. In Proceedings of the IEEE Conference on Computer Vision and Pattern Recognition, Las Vegas, NV, USA, 27–30 June 2016. [CrossRef]
111. Martin, C.; Parkes, S.; Zhang, O.; Zhang, X.; McCabe, M.; Duarte, C. Use of unmanned aerial vehicles for efficient beach litter monitoring. *Mar. Pollut. Bull.* **2018**, *131*, 662–673. [CrossRef]

Disclaimer/Publisher's Note: The statements, opinions and data contained in all publications are solely those of the individual author(s) and contributor(s) and not of MDPI and/or the editor(s). MDPI and/or the editor(s) disclaim responsibility for any injury to people or property resulting from any ideas, methods, instructions or products referred to in the content.